

Article

Not peer-reviewed version

---

# Comprehensive Analysis of Microsatellite Instability in Canine Cancers: Implications for Comparative Oncology and Personalized Veterinary Medicine

---

[Eugenio Mazzone](#) \* and [Luca Aresu](#)

Posted Date: 3 July 2024

doi: [10.20944/preprints202407.0300.v1](https://doi.org/10.20944/preprints202407.0300.v1)

Keywords: Animal Models; Dogs; Cancer; Immunotherapy; Microsatellite Instability; High-Throughput Nucleotide Sequencing



Preprints.org is a free multidiscipline platform providing preprint service that is dedicated to making early versions of research outputs permanently available and citable. Preprints posted at Preprints.org appear in Web of Science, Crossref, Google Scholar, Scilit, Europe PMC.

Copyright: This is an open access article distributed under the Creative Commons Attribution License which permits unrestricted use, distribution, and reproduction in any medium, provided the original work is properly cited.

Disclaimer/Publisher's Note: The statements, opinions, and data contained in all publications are solely those of the individual author(s) and contributor(s) and not of MDPI and/or the editor(s). MDPI and/or the editor(s) disclaim responsibility for any injury to people or property resulting from any ideas, methods, instructions, or products referred to in the content.

## Article

# Comprehensive Analysis of Microsatellite Instability in Canine Cancers: Implications for Comparative Oncology and Personalized Veterinary Medicine

Eugenio Mazzone \* and Luca Aresu

Department of Veterinary Sciences, University of Turin, Turin, Italy

\* Correspondence: eugenio.mazzone@unito.it

**Simple Summary:** This research aims to address the significant knowledge gap regarding microsatellite instability (MSI) in canine cancers. While MSI has been extensively studied in human oncology, its prevalence and importance in canine tumors remain largely unexplored. We seek to provide a comprehensive analysis of MSI across various canine cancer types using a large dataset of whole-exome sequencing samples. By elucidating the landscape of MSI in canine cancers, the study aims to uncover potential implications for cancer development, progression, and treatment strategies. The findings from this research may significantly impact the veterinary oncology community by identifying new biomarkers for prognosis and treatment response, particularly in relation to immunotherapy approaches. Moreover, the study's novel "MSI-burden" score and its correlation with tumor mutational burden could provide valuable insights into canine cancer biology. Ultimately, this research may open new avenues for targeted therapies and personalized medicine in veterinary oncology, potentially improving outcomes for canine cancer patients..

**Abstract:** Microsatellite instability (MSI) is a crucial feature in cancer biology, yet its prevalence and significance in canine cancers remain largely unexplored. This study conducted a comprehensive analysis of MSI across 10 distinct canine cancer histotypes using whole-exome sequencing data from 692 tumor-normal sample pairs. MSI was detected in 64% of tumors, with prevalence varying significantly among cancer types. B-cell lymphomas exhibited the highest MSI burden, contrasting with human studies. A novel "MSI-burden" score was developed, correlating significantly with tumor mutational burden. MSI-high (MSI-H) tumors showed elevated somatic mutation counts compared to MSI-low and microsatellite stable tumors. The study identified 3,632 recurrent MSI-affected genomic regions across cancer types. Notably, seven of the ten cancer types exhibited MSI-H tumors, with prevalence ranging from 1.5% in melanomas to 37% in B-cell lymphomas. These findings highlight the potential importance of MSI in canine cancer biology and suggest opportunities for targeted therapies, particularly immunotherapies. The high prevalence of MSI in canine cancers, especially in B-cell lymphomas, warrants further investigation into its mechanistic role and potential as a biomarker for prognosis and treatment response.

**Keywords:** animal models; dogs; cancer; immunotherapy; microsatellite instability; high-throughput nucleotide sequencing

## 1. Introduction

Microsatellites (MS) are short, tandemly repeated nucleotide sequences dispersed across millions of loci within the genome. Their repetitive nature renders these sequences particularly susceptible to DNA polymerase slippage events during replication, resulting in variations in repeat length [1]. The mismatch repair (MMR) pathway identifies and corrects these errors, thereby safeguarding the genome against potentially deleterious mutations. When the MMR system is compromised, either through genetic mutations or epigenetic silencing, the frequency of spontaneous mutations in microsatellite regions increases, a phenomenon termed microsatellite instability (MSI)[2].



MSI serves as a molecular hallmark of MMR system defects and is associated with various malignancies. It is characterized by the spontaneous gain or loss of nucleotides within these repetitive tracts, indicative of MMR system disruption, leading to the accumulation of somatic mutations at high rates within microsatellites and the formation of novel microsatellite alleles. MSI has significant implications in oncology, particularly in the clinical management of human colorectal and endometrial cancers [3]. Traditionally, molecular investigations of MSI have employed PCR-based methods and immunohistochemistry (IHC) to assess the status of key MMR proteins [4]. However, recent advances in next-generation sequencing (NGS) technologies and computational tools such as mSINGS [5], MSISensor [6], and MANTIS [7] have enabled more comprehensive and precise interrogation of MSI across multiple cancer types. These tools demonstrate high sensitivity and specificity in detecting MSI, broadening the potential for MSI testing beyond the limitations of conventional methods. Emerging evidence suggests that MSI is a generalized feature across a broad spectrum of malignancies [8,9]. Furthermore, MSI has been recognized as an actionable biomarker for immune checkpoint blockade therapies, as patients with MSI-high (MSI-H) tumors respond favorably to inhibitors targeting the programmed cell death protein 1 (PD-1) pathway [10]. This response is likely due to the enhanced recognition of neoantigens by T lymphocytes.

In canine cancers, MSI has been investigated in mammary gland tumors, with 63% of tumors exhibiting a significant MSI degree in 21 microsatellite markers in both blood and tumor tissues [11]. Another study evaluated MMR protein immunolabeling in eight different canine tumors using anti-human monoclonal antibodies [12]. A significant proportion of oral malignant melanomas and hepatocellular carcinomas showed reduced MMR activity, implying possible microsatellite instability. Additionally, a study of 101 dogs with various malignant tumors confirmed that MSI and deregulation of MMR (dMMR) were more prevalent in oral malignant melanomas, demonstrating a correlation between dMMR and MSI [13].

To gain a more comprehensive understanding of MSI prevalence across canine cancers, we utilized msiSensor-pro [14] to analyze MSI status in 10 distinct canine cancer histotypes, encompassing 692 tumors. This analysis was performed on whole exome sequencing data, providing a genome-wide perspective on microsatellite instability. Our study aimed to elucidate the landscape of MSI across a wide array of malignancies and to explore its potential to identify tumors that could benefit from immunotherapy.

## 2. Materials and Methods

### 2.1. Sample Acquisition and Selection Criteria

Samples for this study were obtained from the Sequence Read Archive (SRA) database using the sra-toolkit command-line tool. Twenty studies, encompassing ten distinct canine cancer histotypes, were included in the analysis (Supplementary Table 1). Strict inclusion criteria were applied to ensure robust results. Only paired-end whole-exome sequencing data were considered, with each tumor sample requiring a matched healthy tissue sample from the same animal. Quality control measures were implemented to ensure adequate sequencing coverage.

The canine reference genome (canFam3.1) and corresponding gene annotation were obtained from the University of California, Santa Cruz (UCSC) Genome Browser website. These resources served as the foundation for subsequent analyses and variant calling. To facilitate the identification of somatic variants and minimize false positives, two databases containing known canine germline variants were utilized for filtering: the Dog Single Nucleotide Polymorphism Database (DogSD) [15] and the European Variation Archive (EVA) [16].

### 2.2. Data Preprocessing

The initial phase involved retrieving raw data and comprehensive study metadata, including accession numbers, tumor/normal status, and breed information, from each BioProject's webpage. Python and Bash scripts were used to organize cancer malignancies and matched healthy sequencing data. The Burrows-Wheeler Aligner (BWA) [17] was employed to align each sample to the reference

genome. Despite its somewhat outdated status, CanFam3.1 was chosen as the reference genome due to its widespread use in existing literature, ensuring maximum compatibility with available information. The resulting SAM files underwent processing using SAMtools and Picard tools. Sequencing data were converted to BAM format, enriched with essential metadata, and sorted by coordinate. Finally, base quality score recalibration (BQSR) was performed using the BaseRecalibrator and ApplyBQSR tools from the Genome Analysis Toolkit (GATK) [18] to eliminate possible artifacts and correct quality scores.

### 2.3. Panel of Normals

To mitigate the impact of sequencing artifacts, a Panel of Normals (PON) was created for each analyzed BioProject, comprising mutations called in the corresponding healthy tissues. This approach, following GATK best practices, helped improve the accuracy of mutation identification by filtering out false positives and focusing on true somatic mutations.

### 2.4. Variant Calling

A majority voting approach was employed to identify single nucleotide variants (SNVs) and insertions/deletions (indels), using three callers: Mutect2 [19], Strelka [20], and VarScan [21]. Only aberrations retrieved from at least two out of three callers were considered trustworthy. This approach minimized the impact of caller-specific errors and biases. Annotations were performed using ANNOVAR [22].

### 2.5. Tumor Mutational Burden Analysis

Tumor mutational burden (TMB) was calculated to assess cancer genomic instability. The analysis quantified the total number of mutations per megabase of the coding genome sequenced, excluding mutations in mitochondrial DNA and unaligned chromosomes. The coding regions sequenced were limited to 57Mb, estimated as the size of the canine exome target for each study.

### 2.6. Microsatellite Instability Analysis

msiSensor-Pro [14] was used to perform MSI analysis. Candidate microsatellite regions of interest (ROI) were retrieved from the canFam3.1 reference genome. The tool assessed the number of repeats in the selected loci for all samples, comparing tumor and matched normal data simultaneously. Custom R scripts were used to select the most frequently affected ROI and to model statistical analysis, allowing for the identification of cancer-specific microsatellite instability patterns and their potential associations with other genomic features or clinical outcomes.

## 3. Results

We performed a comprehensive analysis of paired whole-exome sequencing data from 692 tumor-normal sample pairs, encompassing 10 distinct canine cancer subtypes. The sequencing data, obtained from previously published studies, comprised the following distribution: 137 melanomas, 136 mammary carcinomas, 103 B-cell lymphomas, 98 osteosarcomas, 65 T-cell lymphomas, 64 hemangiosarcomas, 52 gliomas, 28 mast cell tumors, 5 pulmonary adenocarcinomas, and 4 urinary carcinomas.

### 3.1. Microsatellite instability

MSI was detected in 446 (64%) tumors across the entire dataset. The prevalence of MSI varied substantially among cancer types, ranging from 100% in pulmonary adenocarcinomas to 29% in T-cell lymphomas. Analysis identified 1,019,895 repeated regions across the tumor sample cohort, distributed across 175,383 unique loci. The frequency of affected loci varied considerably, ranging from a single sample to 117 samples exhibiting alterations at a given locus. Significant differences

( $P<0.001$ ) in the mean number of microsatellite regions were observed among cancer histotypes, ranging from 2.3 in T-cell lymphomas to 19,209 in B-cell lymphomas (Figure 1).

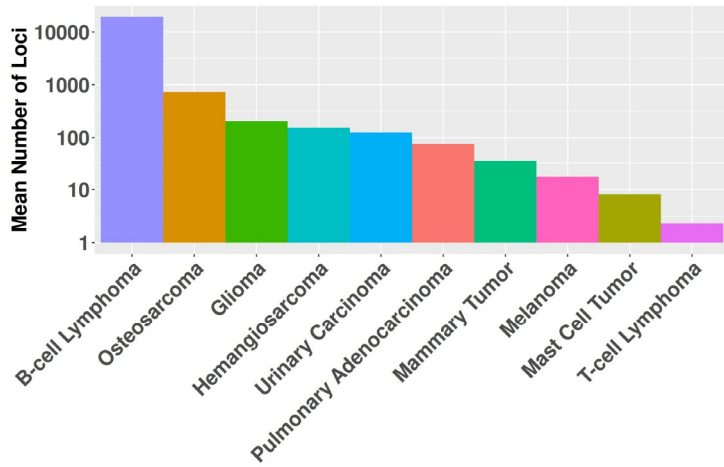


**Figure 1.** The graph displays the mean number of affected loci on a logarithmic scale (y-axis) for each cancer histotype (x-axis).

In the absence of an established consensus for selecting relevant genomic regions to study MSI in canine cancers, we implemented an arbitrary cutoff, retaining loci exhibiting alterations in at least five samples within the whole dataset. B-cell lymphomas were excluded from this analysis step due to their high number of MSI events, which could have obscured relevant loci in other cancer types. We retained 3,632 regions for further analyses (Supplementary Table 2). Evaluation of the entire cohort using these newly identified loci revealed 430 samples harboring at least one MSI event, while 16 samples were excluded due to exhibiting only patient-specific MSI events. The MSI burden of each sample was assessed by calculating the ratio of affected loci to the total number of considered positions (Figure 2). The median MSI burden varied substantially across histotypes, ranging from 19.2% in B-cell lymphomas to 0.05% in T-cell lymphomas. Modeling human MSI categorical classification, we classified tumor histotypes into three categories based on their MSI status: microsatellite stable (MSS) for samples without significant alterations in repeated regions; MSI high (MSI-H) for samples with an MSI burden above the mean value of 2.4%; and MSI low (MSI-L) for samples falling between these categories. Of the 10 cancer types exhibiting MSI, 7 had one or more MSI-H tumors present, with MSI-H prevalence ranging from 1.5% in melanomas to 37% in B-cell lymphomas (Figure 3). The relative level of instability varied considerably among MSI-H cancer types, spanning from 25.8% in B-cell lymphomas to 2.7% in pulmonary adenocarcinomas.

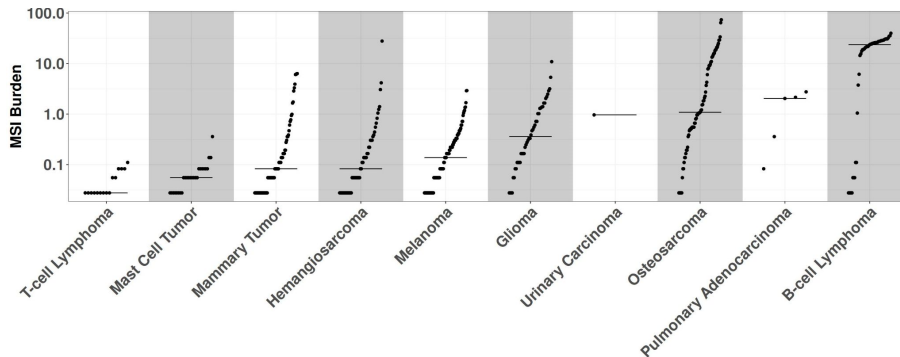


**Figure 2.** The figure displays the MSI burden (y-axis) for each sample by histotype (x-axis). T-cell lymphomas present the lowest while B-cell lymphomas have the highest burden. On the lower part of the figure the number of MSS samples (e.i. burden=0) are visible.

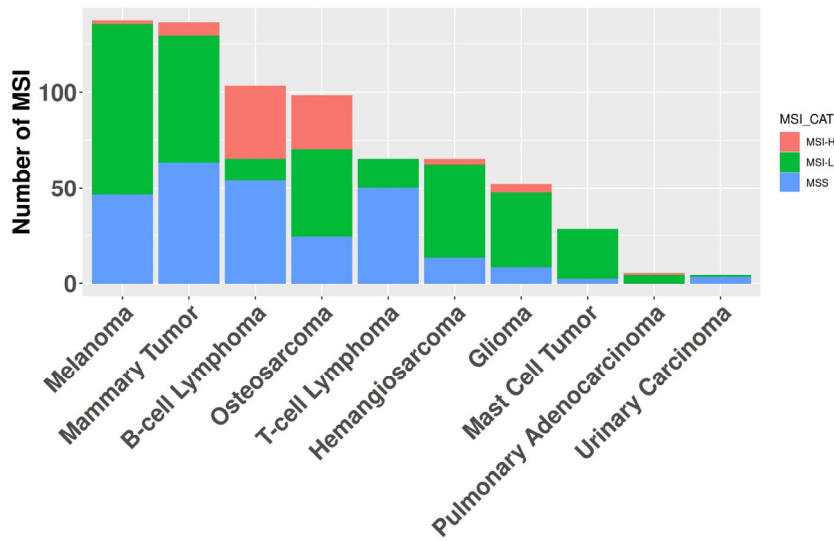


**Figure 3.** The graph depicts the number of samples (y-axis) for each cancer histotype (x-axis). The color-coded bars represent the proportion of tumors within each of the three microsatellite instability (MSI) classifications.

### 3.2. Correlation between Tumor Mutational Burden and MSI Status

Analysis of somatic variants identified through whole-exome sequencing revealed that MSI-H tumors exhibited elevated average absolute numbers of both nonsynonymous and synonymous SNV and indels compared to MSS and MSI-L tumors. Indeed, MSI-H samples harbored a mean of 122 somatic mutations, significantly exceeding the average of 49 somatic mutations observed in MSS samples ( $P < 0.001$ ). MSI-L samples displayed an intermediate mean of 80 somatic mutations, significantly lower than MSI-H ( $P < 0.001$ ) yet higher than MSS ( $P = 0.02$ ), see Figure 4A. To further investigate the relationship between MSI and TMB, defined as the number of coding mutations per megabase sequenced, we assessed TMB across the MSI categories. MSI-H tumors exhibited a mean TMB of 2.14, while MSI-L and MSS tumors showed mean TMB values of 1.43 and 0.89, respectively. MSI-H tumors demonstrated a significantly higher mutational burden compared to both MSI-L and MSS tumors ( $P < 0.001$ ). Moreover, MSI-L tumors exhibited a significantly higher mutational burden than MSS tumors ( $P = 0.043$ ). A visual representation is available in Figure 4B. Linear regression analysis comparing TMB with MSI burden revealed a weak yet statistically significant correlation between these variables ( $R = 0.03$ ,  $P = 0.007$ ), see Figure 5.

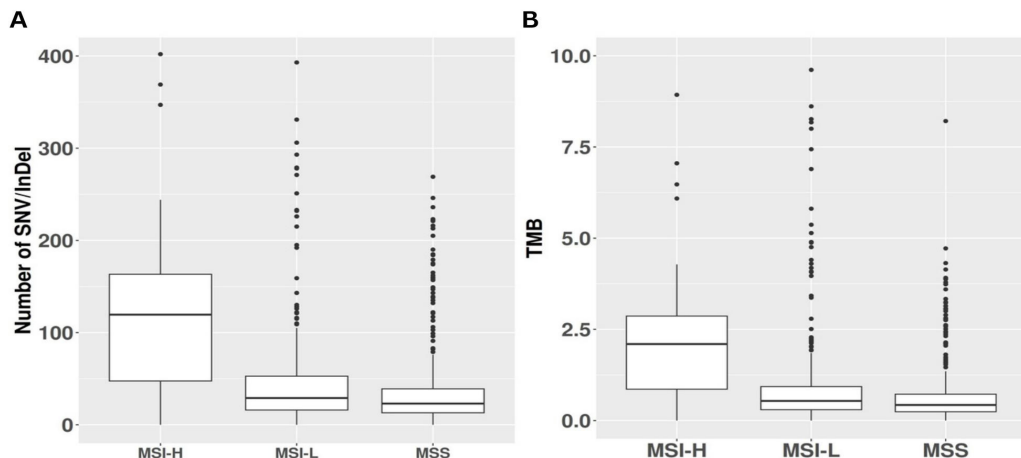


**Figure 4.** This panel illustrates two significant distinctions among microsatellite instability-high (MSI-H), microsatellite instability-low (MSI-L), and microsatellite stable (MSS) tumors, emphasizing the

impact of high MSI levels on the mutational profile. (A) The graph demonstrates the substantial disparity in the number of affected somatic mutations across the three categories. (B) The right graph depicts the variation in TMB among MSI-H, MSI-L and MSS.

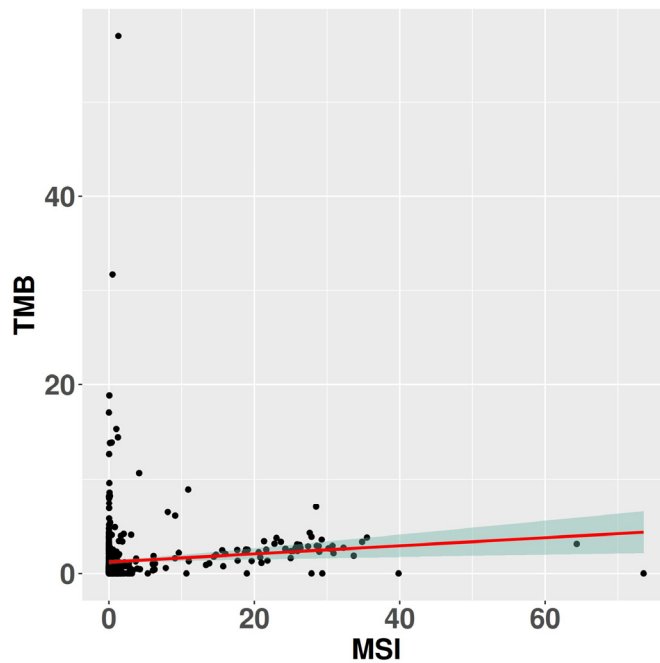


**Figure 5.** The image displays the per-sample correlation between TMB and MSI burden. The red line represents the fitted linear regression function derived from the data.

#### 4. Discussion

MSI is a well-established phenomenon in cancer biology, characterized by the accumulation of mutations in repetitive DNA sequences due to mismatch repair system defects. While extensively studied in human cancers, the prevalence and significance of MSI in canine cancers remain largely unexplored. This study aimed to address this knowledge gap by conducting a comprehensive analysis of MSI in canine cancer exomes, utilizing the largest dataset to date. Our investigation revealed a surprisingly high incidence of MSI, with 430 samples (63%) exhibiting instability. Although sample sizes for certain cancer types, such as pulmonary and urinary carcinomas, were relatively small, potentially affecting the reliability of prevalence estimates, the overall findings underscore the potential importance of MSI in canine cancer development and progression.

Notably, we observed significant heterogeneity in the extent and prevalence of MSI across different canine cancer histotypes. Some histotypes exhibited a high propensity for MSI events, while others displayed a relatively stable microsatellite landscape. Only three cancer types (mast cell tumors, T-cell lymphomas, and urinary carcinomas) did not present at least one MSI-high (MSI-H) sample. Conversely, B-cell lymphoma, osteosarcoma, glioma, mammary tumor, melanoma, hemangiosarcoma, and pulmonary carcinomas displayed higher levels of microsatellite instabilities. The heterogeneity observed across different canine cancer histotypes suggests that MSI may play varying roles in different tumor histologies, similar to what has been observed in human cancers [8]. In human oncology, MSI status has emerged as a powerful biomarker for predicting response to immune checkpoint inhibitors, particularly those targeting the PD-1/PD-L1 axis [10]. The high prevalence of MSI in canine cancers observed in our study suggests that this phenomenon could have significant implications for canine cancer immunotherapy as well. MSI-high tumors are characterized by an increased mutational burden, which can lead to the production of neo-antigens that stimulate an anti-tumor immune response [23]. This increased immunogenicity makes MSI-high tumors particularly susceptible to immune checkpoint inhibition. Given the high prevalence of MSI in canine cancers, there may be a substantial subset of canine cancer patients who could benefit from

immunotherapy approaches targeting PD-1 and PD-L1. Recent studies in canine oncology have begun to explore the potential of immune checkpoint inhibitors. For instance, Maekawa et al. (2017) demonstrated that canine PD-1 and PD-L1 function similarly to their human counterparts, suggesting that targeting this pathway could be effective in canine cancers [23]. Furthermore, Shosu et al. (2016) showed that PD-L1 expression in canine oral melanoma was associated with poor prognosis, mirroring findings in human melanoma [24]. The high prevalence of MSI in canine cancers, coupled with these emerging findings on immune checkpoint molecules, underscores the need for further investigation into the relationship between MSI status and response to immunotherapy in canine patients. Such studies could potentially lead to the development of MSI as a predictive biomarker for immunotherapy response in veterinary oncology, similar to its use in human medicine [24]. Moreover, the cancer-specific variations in MSI prevalence observed in our study suggest that certain canine cancer types may be more amenable to immunotherapy approaches than others. For instance, the high prevalence of MSI in canine B-cell lymphomas and hemangiosarcomas may indicate that these diseases could be particularly responsive to PD-1/PD-L1 blockade.

Notably, the number of MSI affected loci in canine B-cell lymphomas was substantially higher than other canine cancers and previously reported in human studies, where this histotype typically exhibits a low overall MSI burden. This discrepancy may be attributed to the increased sequencing depth of B-cell lymphoma samples compared to other cancer types analyzed in this study. However, given the paucity of data on microsatellite instabilities in canine B-cell lymphomas, further investigation is warranted to elucidate the nature and significance of this phenomenon.

Our large sample size enabled the identification, with reasonable confidence, of the most recurrent genomic locations exhibiting microsatellite instability. We selected 3,632 regions and successfully correlated them with the occurrence of single nucleotide variants and indels, affirming the significance of this aberration family in canine cancers. To classify tumors, we employed a score based on the ratio of MSI-affected loci to the total number of loci of interest. This measure was designed to parallel recent findings in human medicine, where studies have reported a strong correlation between the number of affected loci (and their ratios) and MSI status derived from laboratory techniques such as PCR [7]. We validated the relevance of this "MSI-burden" score by identifying a robust relationship with tumor mutational burden and the number of recurrently somatic mutations, thus revealing the biological implications of our newly defined metric.

Numerous studies in human medicine investigating microsatellite instabilities have employed MANTIS for MSI detection. However, we opted for msiSensor-pro, a more recent computational tool capable of detecting variants in both tumor-normal and tumor-only dataset. Previous performance comparisons between these tools have demonstrated superior results with msiSensor-pro. Moreover, the computation time for msiSensor-pro was significantly lower (approximately 3-4 minutes) compared to MANTIS (around 119 minutes), rendering it a more efficient choice for our analysis.

## 5. Conclusions

In conclusion, this pilot study presents the most comprehensive analysis of MSI in canine cancer exomes across 10 distinct histological subtypes to date. Our findings reveal a surprisingly high overall incidence of MSI and significant heterogeneity across cancer types. These results underscore the potential importance of MSI in canine cancer biology, particularly in B-cell lymphomas, which exhibited the highest MSI burden and introduces a novel "MSI-burden" score, which correlates significantly with TMB and the number of recurrently mutated genes, providing a quantitative measure of MSI impact. These findings have limitations but highlight several key areas for further investigation, including the mechanistic relationship between MSI and canine cancer development, particularly in high-prevalence histotypes, the potential of MSI as a prognostic or predictive biomarker in canine oncology and the correlation between MSI status and response to various treatment modalities, including traditional chemotherapies and targeted therapies. Finally, the high prevalence of MSI in canine cancers suggests a potential opportunity for immunotherapy approaches. Given the success of PD-1 and PD-L1 inhibitors in MSI-high human cancers, investigating these therapies in MSI-high canine cancers represents an exciting frontier in veterinary oncology.

**Supplementary Materials:** The following supporting information can be downloaded at: [www.mdpi.com/xxx/s1](http://www.mdpi.com/xxx/s1), **Table S1:** MS and TMB description for each histotype; **Table S2:** selected *loci* frequently affected by MSI.

**Author Contributions:** Conceptualization, L.A.; methodology, E.M.; software, E.M.; formal analysis, E.M.; data curation, E.M.; writing—review and editing, L.A., E.M.; supervision, L.A. All authors have read and agreed to the published version of the manuscript.

**Funding:** This research received no external funding.

**Informed Consent Statement:** Not applicable.

**Data Availability Statement:** All data are available at <https://github.com/eugeniomazzone/CanineMSI.git> (available after publication).

**Conflicts of Interest:** The authors declare no conflicts of interest.

## References

1. Tautz, D. Notes on the Definition and Nomenclature of Tandemly Repetitive DNA Sequences. *EXS* 1993, 67, 21–28. [https://doi.org/10.1007/978-3-0348-8583-6\\_2](https://doi.org/10.1007/978-3-0348-8583-6_2).
2. Murphy, K.M.; Zhang, S.; Geiger, T.; Hafez, M.J.; Bacher, J.; Berg, K.D.; Eshleman, J.R. Comparison of the Microsatellite Instability Analysis System and the Bethesda Panel for the Determination of Microsatellite Instability in Colorectal Cancers. *J Mol Diagn* 2006, 8, 305–311. <https://doi.org/10.2353/jmoldx.2006.050092>.
3. Imai, K.; Yamamoto, H. Carcinogenesis and Microsatellite Instability: The Interrelationship between Genetics and Epigenetics. *Carcinogenesis* 2008, 29, 673–680. <https://doi.org/10.1093/carcin/bgm228>.
4. Boland, C.R.; Thibodeau, S.N.; Hamilton, S.R.; Sidransky, D.; Eshleman, J.R.; Burt, R.W.; Meltzer, S.J.; Rodriguez-Bigas, M.A.; Fodde, R.; Ranzani, G.N.; et al. A National Cancer Institute Workshop on Microsatellite Instability for Cancer Detection and Familial Predisposition: Development of International Criteria for the Determination of Microsatellite Instability in Colorectal Cancer. *Cancer Res* 1998, 58, 5248–5257.
5. Salipante, S.J.; Scroggins, S.M.; Hampel, H.L.; Turner, E.H.; Pritchard, C.C. Microsatellite Instability Detection by next Generation Sequencing. *Clin Chem* 2014, 60, 1192–1199. <https://doi.org/10.1373/clinchem.2014.223677>.
6. Niu, B.; Ye, K.; Zhang, Q.; Lu, C.; Xie, M.; McLellan, M.D.; Wendl, M.C.; Ding, L. MSIsensor: Microsatellite Instability Detection Using Paired Tumor-Normal Sequence Data. *Bioinformatics* 2014, 30, 1015–1016. <https://doi.org/10.1093/bioinformatics/btt755>.
7. Kutto, E.A.; Bonneville, R.; Miya, J.; Yu, L.; Krook, M.A.; Reeser, J.W.; Roychowdhury, S. Performance Evaluation for Rapid Detection of Pan-Cancer Microsatellite Instability with MANTIS. *Oncotarget* 2017, 8, 7452–7463. <https://doi.org/10.18632/oncotarget.13918>.
8. Bonneville, R.; Krook, M.A.; Kutto, E.A.; Miya, J.; Wing, M.R.; Chen, H.-Z.; Reeser, J.W.; Yu, L.; Roychowdhury, S. Landscape of Microsatellite Instability Across 39 Cancer Types. *JCO Precision Oncology* 2017, 1–15. <https://doi.org/10.1200/PO.17.00073>.
9. Hause, R.J.; Pritchard, C.C.; Shendure, J.; Salipante, S.J. Classification and Characterization of Microsatellite Instability across 18 Cancer Types. *Nat Med* 2016, 22, 1342–1350. <https://doi.org/10.1038/nm.4191>.
10. Le, D.T.; Uram, J.N.; Wang, H.; Bartlett, B.R.; Kemberling, H.; Eyring, A.D.; Skora, A.D.; Luber, B.S.; Azad, N.S.; Laheru, D.; et al. PD-1 Blockade in Tumors with Mismatch-Repair Deficiency. *N Engl J Med* 2015, 372, 2509–2520. <https://doi.org/10.1056/NEJMoa1500596>.
11. McNeil, E.A.; Griffin, K.L.; Mellett, A.M.; Madrill, N.J.; Mickelson, J.R. Microsatellite Instability in Canine Mammary Gland Tumors. *Veterinary Internal Medicine* 2007, 21, 1034–1040. <https://doi.org/10.1111/j.1939-1676.2007.tb03061.x>.
12. Sotirakopoulos, A.J.; Armstrong, P.J.; Heath, L.; Madrill, N.J.; McNeil, E.A. Evaluation of Microsatellite Instability in Urine for the Diagnosis of Transitional Cell Carcinoma of the Lower Urinary Tract in Dogs: Microsatellite Instability in TCC. *Journal of Veterinary Internal Medicine* 2010, 24, 1445–1451. <https://doi.org/10.1111/j.1939-1676.2010.0617.x>.
13. Inanaga, S.; Igase, M.; Sakai, Y.; Tanabe, M.; Shimonohara, N.; Itamoto, K.; Nakaichi, M.; Mizuno, T. Mismatch Repair Deficiency in Canine Neoplasms. *Vet Pathol* 2021, 58, 1058–1063. <https://doi.org/10.1177/03009858211022704>.
14. Jia, P.; Yang, X.; Guo, L.; Liu, B.; Lin, J.; Liang, H.; Sun, J.; Zhang, C.; Ye, K. MSIsensor-Pro: Fast, Accurate, and Matched-Normal-Sample-Free Detection of Microsatellite Instability. *Genomics, Proteomics & Bioinformatics* 2020, 18, 65–71. <https://doi.org/10.1016/j.gpb.2020.02.001>.
15. Bai, B.; Zhao, W.-M.; Tang, B.-X.; Wang, Y.-Q.; Wang, L.; Zhang, Z.; Yang, H.-C.; Liu, Y.-H.; Zhu, J.-W.; Irwin, D.M.; et al. DoGSD: The Dog and Wolf Genome SNP Database. *Nucleic Acids Res* 2015, 43, D777–D783. <https://doi.org/10.1093/nar/gku1174>.

16. Cezard, T.; Cunningham, F.; Hunt, S.E.; Koylass, B.; Kumar, N.; Saunders, G.; Shen, A.; Silva, A.F.; Tsukanov, K.; Venkataraman, S.; et al. The European Variation Archive: A FAIR Resource of Genomic Variation for All Species. *Nucleic Acids Res* 2022, 50, D1216–D1220. <https://doi.org/10.1093/nar/gkab960>.
17. Li, H.; Durbin, R. Fast and Accurate Long-Read Alignment with Burrows-Wheeler Transform. *Bioinformatics* 2010, 26, 589–595. <https://doi.org/10.1093/bioinformatics/btp698>.
18. McKenna, A.; Hanna, M.; Banks, E.; Sivachenko, A.; Cibulskis, K.; Kernytsky, A.; Garimella, K.; Altshuler, D.; Gabriel, S.; Daly, M.; et al. The Genome Analysis Toolkit: A MapReduce Framework for Analyzing next-Generation DNA Sequencing Data. *Genome Res.* 2010, 20, 1297–1303. <https://doi.org/10.1101/gr.107524.110>.
19. Cibulskis, K.; Lawrence, M.S.; Carter, S.L.; Sivachenko, A.; Jaffe, D.; Sougnez, C.; Gabriel, S.; Meyerson, M.; Lander, E.S.; Getz, G. Sensitive Detection of Somatic Point Mutations in Impure and Heterogeneous Cancer Samples. *Nat Biotechnol* 2013, 31, 213–219. <https://doi.org/10.1038/nbt.2514>.
20. Kim, S.; Scheffler, K.; Halpern, A.L.; Bekritsky, M.A.; Noh, E.; Källberg, M.; Chen, X.; Kim, Y.; Beyter, D.; Krusche, P.; et al. Strelka2: Fast and Accurate Calling of Germline and Somatic Variants. *Nat Methods* 2018, 15, 591–594. <https://doi.org/10.1038/s41592-018-0051-x>.
21. Koboldt, D.C.; Zhang, Q.; Larson, D.E.; Shen, D.; McLellan, M.D.; Lin, L.; Miller, C.A.; Mardis, E.R.; Ding, L.; Wilson, R.K. VarScan 2: Somatic Mutation and Copy Number Alteration Discovery in Cancer by Exome Sequencing. *Genome Res.* 2012, 22, 568–576. <https://doi.org/10.1101/gr.129684.111>.
22. Wang, K.; Li, M.; Hakonarson, H. ANNOVAR: Functional Annotation of Genetic Variants from High-Throughput Sequencing Data. *Nucleic Acids Research* 2010, 38, e164. <https://doi.org/10.1093/nar/gkq603>.
23. Llosa, N.J.; Cruise, M.; Tam, A.; Wicks, E.C.; Hechenbleikner, E.M.; Taube, J.M.; Blosser, R.L.; Fan, H.; Wang, H.; Luber, B.S.; et al. The Vigorous Immune Microenvironment of Microsatellite Instable Colon Cancer Is Balanced by Multiple Counter-Inhibitory Checkpoints. *Cancer Discov* 2015, 5, 43–51. <https://doi.org/10.1158/2159-8290.CD-14-0863>.
24. Marcus, L.; Lemery, S.J.; Keegan, P.; Pazdur, R. FDA Approval Summary: Pembrolizumab for the Treatment of Microsatellite Instability-High Solid Tumors. *Clin Cancer Res* 2019, 25, 3753–3758. <https://doi.org/10.1158/1078-0432.CCR-18-4070>. Author 1, A.; Author 2, B. Title of the chapter. In *Book Title*, 2nd ed.; Editor 1, A., Editor 2, B., Eds.; Publisher: Publisher Location, Country, 2007; Volume 3, pp. 154–196.

**Disclaimer/Publisher's Note:** The statements, opinions and data contained in all publications are solely those of the individual author(s) and contributor(s) and not of MDPI and/or the editor(s). MDPI and/or the editor(s) disclaim responsibility for any injury to people or property resulting from any ideas, methods, instructions or products referred to in the content.